Proceedings of the 6th International Conference on Gas Hydrates (ICGH 2008),
Vancouver, British Columbia, CANADA, July 6-10, 2008.

ANALYSES OF PRODUCTION TESTS AND MDT TESTS CONDUCTED IN MALLIK AND ALASKA METHANE HYDRATE RESERVOIRS: WHAT CAN WE LEARN FROM THESE WELL TESTS?

Masanori Kurihara*, Kunihiro Funatsu and Hisanao Ouchi
Japan Oil Engineering Company
1-7-3 Kachidoki, Chuo-ku, Tokyo, 104-0054, Japan

Yoshihiro Masuda (School of Engineering, The University of Tokyo)

Koji Yamamoto (Japan Oil, Gas and Metals National Corporation)

Hideo Narita (National Institute of Advanced Industrial Science and Technology)

Scott R. Dallimore (Geological Survey of Canada, Natural Resources Canada)

Timothy S. Collett (United States Geological Survey)

Steve H. Hancock (APA Petroleum Engineering Inc.)

ABSTRACT

Pressure drawdown tests were conducted using Schlumberger's Modular Formation Dynamics Tester™ (MDT) wireline tool in the Mallik methane hydrate (MH) reservoirs in February 2002 as well as in the Mount Elbert (Alaska) MH reservoirs in February 2007, while a production test was conducted applying a depressurization method in one of the Mallik MH reservoirs in April 2007. All of these tests aimed at measuring production and bottomhole pressure (BHP) responses by reducing BHP below the MH stability pressure to estimate reservoir properties such as permeability and MH dissociation radius. We attempted to analyze the results of these tests through history matching using the numerical simulator (MH21-HYDRES) coded especially for gas hydrate reservoirs. Although the magnitude of depressurization and the total duration spent for these tests were almost identical to each other, the simulation studies revealed that there existed significant differences in what could be inferred and could not be inferred from test results between a MDT test and a production test.

The simulation studies mainly clarified that (1) the MDT tests were useful to estimate initial effective permeability in the presence of MH, (2) when BHP is reduced below the MH stability pressure at MDT tests, the pressure and temperature responses were significantly influenced by the wellbore storage erasing all the important data such as those indicating a radius of MH dissociation and effective permeability after partial MH dissociation, and (3) history matching of production tests tended to result in multiple solutions unless establishing steady flow conditions.

This paper presents the results of history matching for the typical MDT and production tests conducted in Mallik and Alaska MH reservoirs. This paper also discusses the parameters reliably estimated through MDT and production tests, which should provide many suggestions on future designs and analyses of short-term tests for MH reservoirs.

Keywords: MDT, production test, numerical simulation, history matching

* Corresponding author: Phone: +81 3 5548 1663 Fax: +81 3 5548 1673 Email: kurihara@joe.co.jp

NOMENCLATURE

B formation volume factor [m^3/m^3]
c compressibility [1/Pa]
D depth [m]
g gravity acceleration [m/s^2]
h thickness [m]
k absolute permeability [m^2]
k_e effective permeability [m^2]
k_r relative permeability
p pressure [Pa]
q fluid production rate [m^3/s]
$\tilde{q}$ fluid injection rate per unit reservoir bulk volume [m^3/s]
r radial dimension [m]
S fluid saturation
t time [s]
μ viscosity [Pa-s]
ρ density [kg/m^3]
ϕ porosity

subscript
g gas
init initial
R rock
t total
w water
well wellbore

INTRODUCTION

In the Mallik 2002 Gas Hydrate Production Research Well Program [1], formation tests with the MDT tool were conducted at the JAPEX/JNOC/GSC et al. Mallik 5L-38 well to measure the production rates from test intervals in response to reducing the bottomhole flowing pressure and to infer reservoir properties from the flow and pressure data [2]. The test results were then analyzed using conventional pressure transient test analysis methods [3], which are widely applied to analyze test results in conventional oil and gas reservoirs [4, 5]. One of these MDT test results were also analyzed using the numerical simulator (MH21-HYDRES) coded especially for gas hydrate reservoirs, which attempted to estimate the reservoir properties through history matching simulation [6].

Another series of MDT tests was conducted in February 2007 by the U.S. Department of Energy, BP Exploration (Alaska) and the U.S. Geological Survey, in order to collect the first open-hole formation pressure response data in the MH reservoir (the "Mount Elbert" stratigraphic test well). As part of an ongoing effort to compare the world's leading gas hydrate reservoir simulators including MH21-HYDRES, an international group conducted history matches of one 12-hour MDT test [7].

On the other hand, the gas hydrate production test was conducted using the depressurization methods in the JOGMEC/NRCan/Aurora Mallik production program in April 2007, aiming at the continuous MH dissociation and production [8]. The results of this production test were analyzed, based on all the data acquired during the test, using MH21-HYDRES [9].

The effort for analyzing these MDT tests and the production test suggested the difficulties in estimation of reservoir properties such as the effective permeability to gas and water and the radius of MH dissociation. This paper briefly review the results of the analyses for the past MDT and production tests and also discusses the parameters reliably estimated through MDT tests and production tests, which should provide many suggestions on future designs and analyses of short term tests for MH reservoirs.

NUMERICAL SIMULATOR

The Research Consortium for Methane Hydrate Resources in Japan (MH21 Research Consortium), which was organized to attain the exploration and exploitation of MH offshore Japan, has been implementing a variety of research projects toward the assessment of MH resources, establishment of MH production methods and examination of the impact of MH development on the environment. As part of such research projects, we have been developing the state-of-the-art numerical simulator (MH21-HYDRES) for rigorously predicting MH dissociation and production behaviors both at core and field scales. This simulator has a capability to deal with 3-D, 5-phase and 4-component problems associated with MH dissociation kinetics. Further details on this simulator are given in our previous papers [10, 11, 12, 13].

THEORY OF PRESSURE TRANSIENT TEST ANALYSIS

The derivation of the equations used in the traditional pressure transient test analysis is briefly summarized below [4, 5].

In general, the flow of a certain fluid in a porous medium is expressed rigorously as [14]

$$\nabla \cdot \left[\frac{k k_r}{\mu B} \left(\nabla p + \rho g \nabla D \right) \right] + \tilde{q} = \frac{\partial}{\partial t} \left(\frac{S \phi}{B} \right). \tag{1}$$

In conventional well test analysis methods, assuming that the rock and fluid properties are independent of time and space throughout the test period and that the fluid flows in the single-phase state without the effect of gravity and under a small pressure gradient, Equation (1) is simplified to [4]

$$\frac{k}{\phi \mu c_t} \nabla^2 p = \frac{\partial p}{\partial t}, \tag{2}$$

where c_t denotes a total compressibility given by $c_t = c_f + c_R$. For the radial flow expected in a well test, Equation (2) is further reduced to

$$\frac{1}{r} \frac{\partial}{\partial r} \left(r \frac{\partial p}{\partial r} \right) = \frac{\phi \mu c_t}{k} \frac{\partial p}{\partial t}. \tag{3}$$

For gas-water two-phase flow, which is the most likely flow condition expected during a well test in a MH reservoir, Equations (1) for the gas and water phases are combined mathematically, ignoring the capillary pressure, saturation gradient and generation of gas and water, to yield

$$\frac{1}{r} \frac{\partial}{\partial r} \left(r \frac{\partial p}{\partial r} \right) = \frac{\phi c_t}{\left(\frac{k_e}{\mu} \right)_t} \frac{\partial p}{\partial t}, \tag{4}$$

where the total compressibility c_t and the total mobility $\left(\frac{k_e}{\mu} \right)_t$ are defined, neglecting the dissolution of gas into water, as

$$c_t = -\frac{S_w}{B_w} \frac{\partial B_w}{\partial p} - \frac{S_g}{B_g} \frac{\partial B_g}{\partial p} + c_R = S_w c_w + S_g c_g + c_R \tag{5}$$

$$\left(\frac{k_e}{\mu} \right)_t = k \left(\frac{k_{rw}}{\mu_w} + \frac{k_{rg}}{\mu_g} \right). \tag{6}$$

Equation (3) can be analytically solved assuming a constant production rate of q with appropriate initial and boundary conditions, such as those for an infinitely acting reservoir, bounded circular reservoir, and constant-pressure outer boundary. For example, in an infinitely acting reservoir, the initial and boundary conditions are defined as

$$p = p_{init}, \quad \text{for all } r \text{ at } t = 0 \quad (\text{initial condition}) \tag{7}$$

$$p \to p_{init}, \quad \text{for } r \to \infty \text{ at } t > 0 \quad (\text{boundary condition}) \tag{8}$$

$$\frac{\partial p}{\partial r} = \frac{q \mu B}{2 \pi k h r_{well}}, \quad \text{for } r = r_{well} \text{ at } t > 0 \quad (\text{boundary condition}). \tag{9}$$

The solution of Equation (3) is then given by the following exponential-integral equation, when $\frac{kt}{\phi \mu c_t r^2} \geq 25$:

$$p(r,t) = p_{init} - \frac{q \mu B}{2 \pi k h} \left[-\frac{1}{2} \mathrm{Ei} \left(-\frac{\phi \mu c_t r^2}{4kt} \right) \right], \tag{10}$$

where the exponential-integral is defined by

$$\mathrm{Ei}(-x) = -\int_x^\infty \frac{e^{-u}}{u} du. \tag{11}$$

When $\frac{kt}{\phi \mu c_t r^2} > 100$, Equation (10) is approximated as

$$p(r,t) = p_{init} - \frac{q \mu B}{4 \pi k h} \left[\ln \left(\frac{kt}{\phi \mu c_t r^2} \right) + 0.80907 \right], \tag{12}$$

which is applied most popularly to the conventional pressure transient test analysis methods.

The solution of Equation (4) can be also given in the same manner as the above. Since Equations (3) and (4) are linear and homogeneous, the superposition of the solutions with simple

boundary conditions in time and space leads to the solutions with the complicated boundary conditions, such as those associated with the multiple rates and multiple wells.

NUMERICAL EXPERIMENTS FOR INVESTIGATING THE APPLICABILITY OF CONVENTIONAL WELL TEST ANALYSIS METHODS TO MDT TESTS IN MH RESERVOIRS

Although MH saturation, and hence effective permeability to fluids, significantly change along with the dissociation of MH during the test in a MH reservoir, reservoir parameters such as permeability and distances to boundaries are assumed to be constant and are estimated in accordance with the solutions of Equation (3) or (4) (e.g., that given by Equation (12)), whenever conventional pressure transient test analysis methods are applied. Therefore, where MH saturation changes are large during the course of a well test, it is difficult to assess the reliability and certainty of conventional well test analysis methods in determining a single average value for the well test parameters.

A series of numerical experiments were conducted to investigate how the solutions of Equation (3) or (4), therefore the conventional well test analysis methods, could be applied to the analyses of MDT test behavior in MH reservoirs. It was also examined through these experiments how the estimates of reservoir properties such as permeability and the distances to the boundary by the conventional methods are close to those assigned to the numerical models [6].

Procedure of numerical experiments

A one-dimensional radial MH reservoir model was constructed, in accordance with the specifications listed in Table 1, targeting the vicinity of a hypothetical well where MDT tests are conducted. The reservoir properties such as porosity, absolute permeability and initial pressure and temperature were assigned to the model so as to make it similar to the Mallik reservoir where the actual MDT tests were conducted.

The MDT test behaviors were simulated with this model, assuming a variety of reservoir properties such as initial MH saturation and permeability reduction exponent. Pressure responses were predicted in accordance with the schedule of two sets of pressure drawdown-buildup (1-hour first flow at a constant total fluid production rate of 0.173 m^3/d, 3-hour first shut-in, 1-hour second flow at a constant total fluid production rate of 0.432 m^3/d and 5-hour second shut-in). These simulation-derived pressure responses are then examined by conventional well test methods as illustrated in Figure 1.

Model area	500 m radius in the vicinity of the well
Thickness	1 m
Grid system	50 x 1 x 1 (radial)
Grid size (Δr)	0.020, 0.024, 0.028, ..., 77.7 m (max. r = 500 m)
Wellbore radius	0.108 m (8.5 inches)
Absolute permeability	1000 mD
Porosity	38%
Initial pressure	9.3 MPa
Initial temperature	286 K

Table 1: Specifications of radial model for numerical experiments

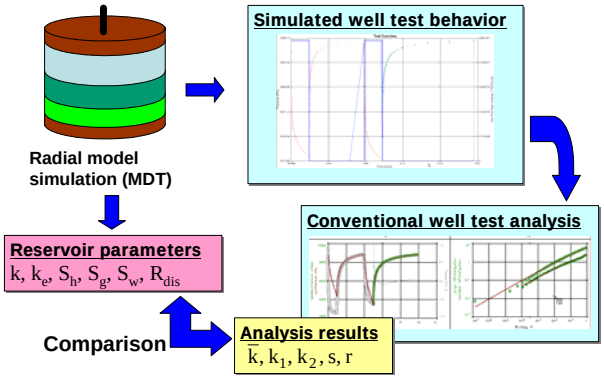

Figure 1: Procedure of numerical experiments

Analyses assuming infinitely acting model

The simulated bottomhole pressure behavior at the second shut-in was analyzed based on water production rates, using an infinitely acting reservoir model solution with a zero skin factor. Figure 2 shows the log-log plots, along with the analytical solution curves with appropriate permeability, for initial MH saturations of 70 and 90%. Note that the difference between the simulated pressure and optimal analytical solution is significant in the case of the initial MH saturation of 90%, which indicates the limitation of the applicability of the infinitely acting model. As summarized in Table 2, the calculated effective permeabilities to water suggested by these analytical curves are 3.12 and 0.05 mD for initial MH saturations of 70 and 90%, respectively.

On the other hand, the predicted effective permeabilities to water at the short radius (where the minimum MH saturation is detected after the second flow), medium radius (where the MH saturation is equal to the average MH saturation over the MH dissociation area) and long radius (where the MH saturation is less than the initial MH saturation by 1%), as listed in Table 2, indicate that the effective permeability to water estimated by conventional well test analysis methods is similar to that at the medium radius distance.

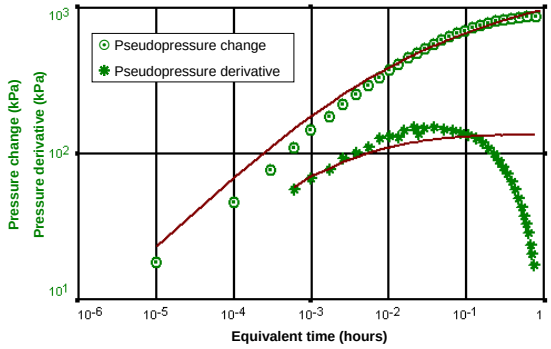

(a) Initial MH saturation of 70%

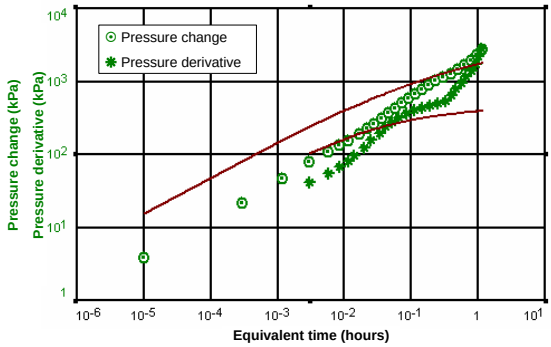

(b) Initial MH saturation of 90%

Figure 2: Log-log plots of pressure and pressure derivative with analytical solution lines

Model initial condition	S_H	0.7			0.9		
	k_{ew} (mD)	2.43			0.01		
Model parameters after 2nd flow	Radial portion	Short	Medium	Long	Short	Medium	Long
	r (m)	0.1179	0.1383	1.7508	0.1179	0.2719	0.4542
	S_H	0.6423	0.6725	0.6988	0.6109	0.8738	0.8990
	S_g	0.0231	0.0202	0.0017	0.0884	0.0109	0.0039
	S_w	0.3346	0.3073	0.2995	0.3007	0.1153	0.0972
	k^* (mD)	5.8584	3.7690	2.4782	8.9230	0.0320	0.0105
	k_{rw}	0.7770	0.7859	0.9792	0.3669	0.7090	0.8630
	$k_{ew}=k^*k_{rw}$ (mD)	4.5519	2.9622	2.4266	3.2739	0.0227	0.0091
Analysis results	k (mD)	3.1220			0.0530		
	k/k_{ew}	0.6859	1.0539	1.2866	0.0162	2.3359	5.8354

Table 2: Comparison of numerical model parameters and those analyzed by infinitely acting model

Analyses assuming other models

Since the bottomhole pressure behavior for initial MH saturations of 80% or less indicates the existence of a constant pressure boundary (CPB) or no-flow boundary (NFB) and that for initial MH saturation of 90 % shows the trend diagnostic of laterally decreasing permeability, these pressure behaviors were analyzed using other models in an attempt to find a better matched solution and information on the radius of MH dissociation. As shown in Table 3 and Figure 3, the calculated permeability derived from other models is not significantly different from that estimated by the infinitely acting reservoir model for many of the initial MH saturations, although the analytical solutions from some of these models show much better agreement with the simulated bottomhole pressure behaviors as shown in Figure 3.

Initial hydrate saturation	Radial portion	Radius (m)	Effective permeability to gas (mD)	Analysis results					
				CPB model		NFB model		Composite model	
				k_{ew} (mD)	R (m)	k_{ew} (mD)	R (m)	k_{ew} (mD)	R (m)
0.4	S, M, L	0.118	77.670	79.701	11.214	79.215	15.350	78.930	14.250
0.5	S, M, L	0.118	31.334	34.472	6.483	32.160	10.000	32.058	9.400
0.6	S, M, L	0.118	11.160	11.088	3.913	10.931	6.560	10.895	6.170
0.7	S	0.118	4.552	3.087	1.795	2.966	4.830	2.988	4.550
	M	0.138	2.962						
	L	1.751	2.427						
0.8	S	0.118	3.478	0.660	1.755	0.639	11.190	0.639	9.530
	M	0.231	0.612						
	L	1.249	0.319						
0.9	S	0.118	3.274	0.055	0.895	0.052	4.240	0.105	0.380
	M	0.272	0.023						
	L	0.454	0.009						

Abbreviations: S, short radius; M, medium radius; L, long radius; CPB, constant-pressure boundary; NFB, no-flow boundary; R, distance to boundary

Table 3: Comparison of numerical model parameters and those analyzed by various models

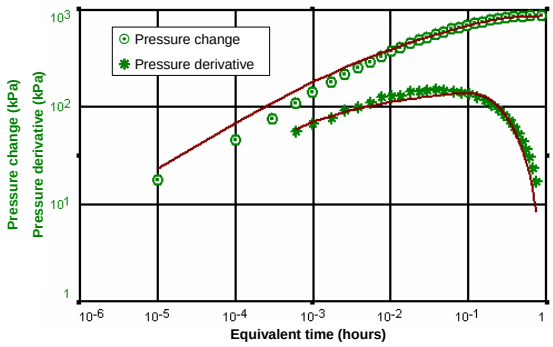

(a) Initial MH saturation of 70% (constant pressure boundary model)

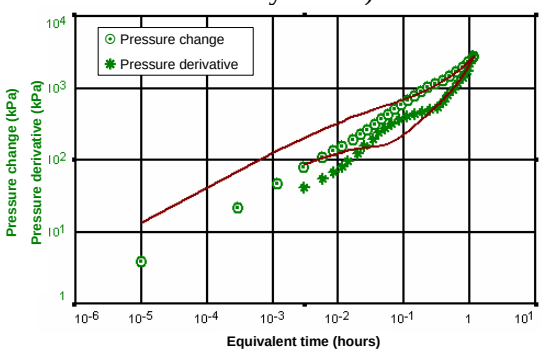

(b) Initial MH saturation of 90% (composite model)

Figure 3: Log-log plots of pressure and pressure derivative with analytical solution lines

For initial MH saturation of 90%, the boundary to the permeability reduction estimated by the composite model may suggest the medium or long radius. For initial MH saturations of 70 and 80%, the estimated distances to a CPB seem to indicate the long radii. For initial MH saturations of less than 70%, however, the distances suggested by the models accounting for these boundaries are far greater than those observed in the simulation models and are not appropriate for inferring radii of MH dissociation, as shown in Table 3.

ANALYSES OF MDT TEST IN MALLIK

The second MDT test actually conducted on the Mallik 5L-38 well in February 2002 [3], for the interval between 1089.5 and 1090.0 m, was reproduced through numerical simulation to examine how the actual well test analysis was effective at inferring MH reservoir parameters [6]. This MDT test was composed of two parts, namely a production–shut-in part and an injection–shut-in part, as shown in Figure 4. The first part of the test was selected as the target for the simulation and examination.

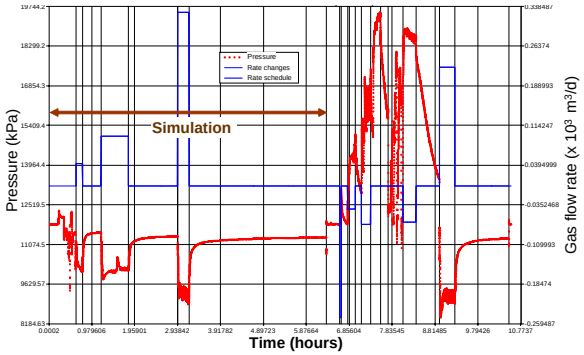

Figure 4: MTD test#2 performances

Note that the gas flow rate shown in Figure 4 were estimated based simply on the bottomhole pumping rates assuming that only gas flowed from the reservoir [3].

Reservoir modeling

As shown in Table 4 and Figure 5, the two-dimensional radial model was constructed to replicate the interval where MDT test#2 was actually carried out. In the model, the test interval of 0.5 m was divided into five grid layers, only the centre (third) layer of which was assumed to connect with the well by perforation. The reservoir properties, such as porosity and MH saturation, were assigned to the model in accordance with the well log interpretation results [14]. Note that the wellbore storage effect was neglected and that the fluid flow was assumed to stop at the sand face instantaneously after shut-in.

Model area	500 m in the vicinity of the well
Thickness	1.2 m
Grid system	50 x 1 x 7 (radial)
Grid size (Δr)	0.020, 0.024, 0.028, ..., 77.7 m (max. r = 500 m)
Wellbore radius	0.108 m (8.5 inches)
Absolute permeability	400 mD
Porosity	41.5%
Permeability reduction index (N)	3
Initial gas hydrate saturation	85.1%
Initial water saturation	14.9%
Initial pressure	11.568 MPa
Initial temperature	287.05 K

Table 4: Specifications of radial model for history matching of Mallik MDT test behavior

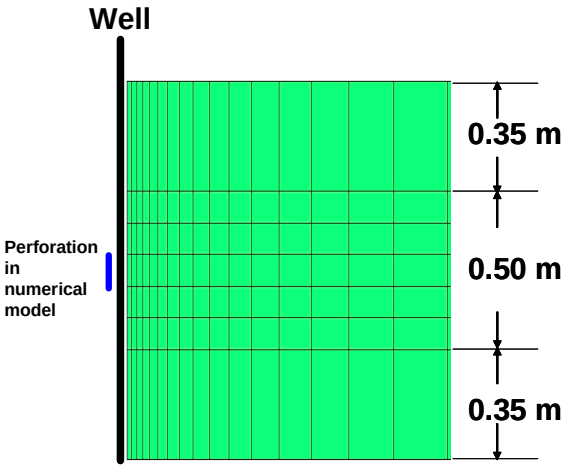

Figure 5: MTD test#2 performances

History matching

Figure 6 (a) depicts the bottomhole pressure simulated with the above model specifying the total fluid rate (pumping rate) as a boundary condition, together with the actual bottomhole pressure observed during the test. There is a significant difference between the observed and simulated pressures, especially for the second and third flows. The parameters of the reservoir model, especially absolute and relative permeabilities, were then adjusted to reproduce the observed bottomhole pressure [6]. As shown in Figure 6 (b),

a satisfactory agreement between observed and simulated pressure behavior was accomplished. The production rates of gas and water during the test, and the distribution of MH saturation after the third flow period, simulated with the history matched model are given in Figures 7 and 8, respectively. It was inferred that the gas flow was not dominant at the bottomhole even during the third flow period and that the medium and long radii after the third flow were as small as about 0.171 and 0.408 m, respectively.

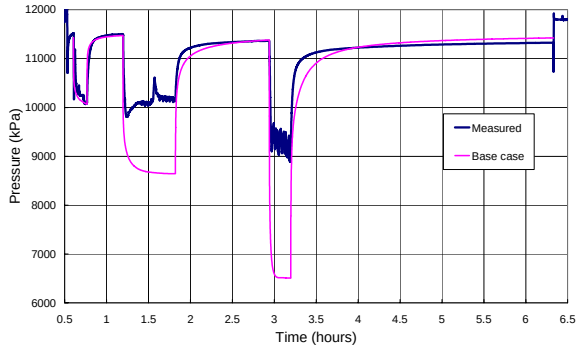

(a) Initial run

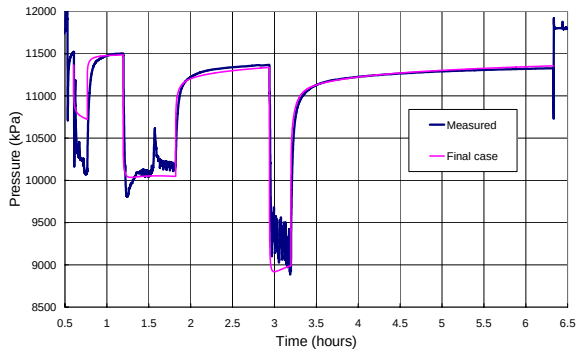

(b) History matched

Figure 6: Simulated bottomhole pressure behavior

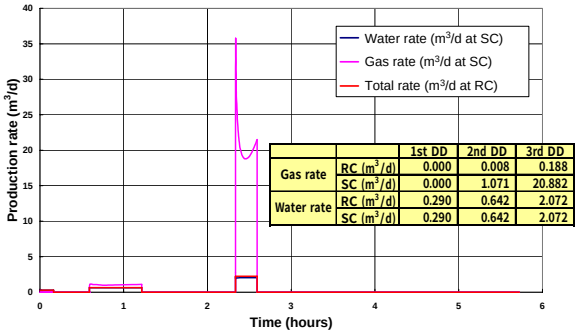

		1st DD	2nd DD	3rd DD
Gas rate	RC (m^3/d)	0.000	0.008	0.188
	SC (m^3/d)	0.000	1.071	20.882
Water rate	RC (m^3/d)	0.290	0.642	2.072
	SC (m^3/d)	0.290	0.642	2.072

Figure 7: Simulated gas and water flow rates

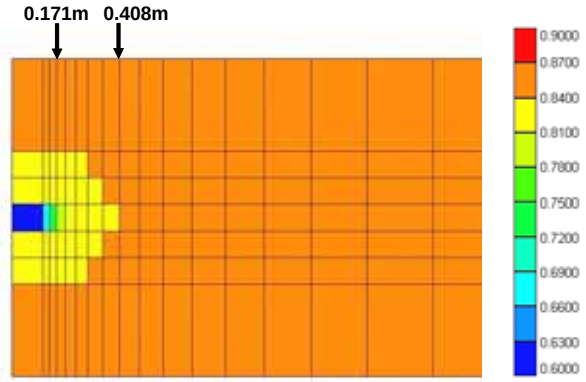

Figure 8: Simulated MH saturation distribution after third flow

Examination of actual analysis results

The parameters of the history matched model were then compared to the actual MDT test analysis results. Figure 9 shows the log-log plot of pressure and pressure derivative for the third shut-in period, simulated with the history matched model, together with the measured values. Although there is a noteworthy difference between the simulated and measured values in the very early part of the shut-in, the match could have been significantly improved if a wellbore-storage coefficient was incorporated into the simulation. The simulated pressure derivative behavior corresponding to the medium radius is masked due either to too small elapsed shut-in time or to the effect of partial penetration. The simulated pressure derivative at the middle part of the shut-in depicts the normal radial flow followed by the indication of a lateral decrease in permeability beyond the long radius. The simulated pressure derivative drastically increases during the late part of the shut-in, similar to the analytical model with sealing faults or laterally decreasing permeability.

On the other hand, the measured pressure derivative plots on a unit slope line during the early part of the shut-in, indicating a dominant wellbore storage effect, then deviates from this line and becomes constant, depicting a radial flow portion of the buildup. Finally, the measured pressure derivative significantly increases during the late part of the shut-in, indicating the presence of sealing faults or laterally decreasing permeability.

Table 5 summarizes the reservoir parameters analyzed using conventional well test analysis method with sealing faults, as well as those

observed in the history matched model. For the third shut in period, the effective permeability to water was analyzed to be about 33 mD assuming 100% of water flow, which is very similar to 39 mD predicted at the middle radius in the history matched model. On the other hand, the effective permeability to gas was analyzed to be 0.1 mD assuming 100% of gas flow, while that observed in the history matched model is much smaller. This difference must result from the assumption of 100% gas flow and from the application of gas properties for the fluid physical properties of viscosity, formation volume factor and compressibility to the analysis. The effective permeability to gas is corrected to be 0.07 mD by applying the gas production rate shown in Figure 7 and the properties of the gas-water mixture, which is a good estimate of the effective permeability at the short or medium radius obtained from the modeling. However, it should be noted that the accurate estimation of gas and water rates at the bottomhole is very difficult, as no fluid flows to the surface.

Since the shut-in time corresponding to the long radius was masked by wellbore-storage effects in the actual test, NFB like actual pressure response suggests not the radius of MH dissociation but the sealing faults or laterally decreasing permeability, probably caused by the significant permeability reduction associated with the change in facies or MH characteristics. Since this distance to the boundary was calculated based on the effective permeability to gas and the physical properties of gas in the actual test analysis, it was estimated to be as low as 0.8 m, which is much smaller than 7.3 m estimated from the history matching simulation.

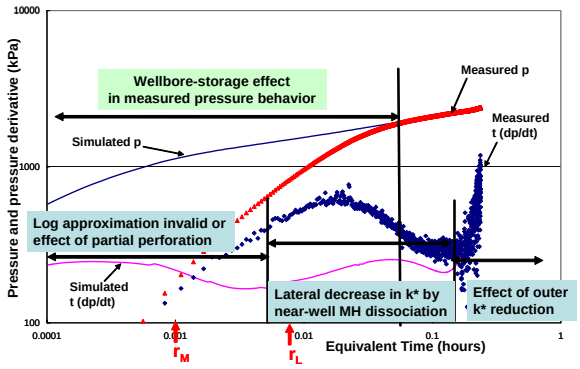

Figure 9: Log-log plots of pressure and pressure derivative, comparing simulated and measured data

			1st BU	2nd BU	3rd BU
Analysis results	k_{eg} (mD)		0.029	0.067	0.100
	L_b (m)		-	-	0.812
	k_{ew} (mD)		2.000	5.192	32.639
	k_{eg} corrected with Q, μ, c_t		0.000	0.00727	0.0722
Model parameters	Absolute permeability (mD)		2000–4000		
	k_{eg} (mD)	S	0.000	0.00526	0.0912
		M	0.000	0.00203	0.0184
		L	0.000	0.00062	0.0045
	k_{ew} (mD)	S	8.151	49.487	190.258
		M	8.151	22.058	39.180
		L	8.151	11.885	11.735
	Gas hydrate dissociation radius (m)	S	0.000	0.119	0.119
		M	0.000	0.143	0.171
		L	0.000	0.204	0.408
	Distance to boundary (m)		7.328	7.328	7.328

Abbreviations: S, short radius; M, medium radius; L, long radius; L_b, distance to boundary Q, production rate; μ, viscosity; c_t, total compressibility; BU, buildup

Table 5: Comparison between history matched model parameters and analyzed parameters

ANALYSES OF MDT TEST IN MT ELBERT

MDT tests were conducted in the Mt Elbert MH reservoirs in February 2007. The first through the third flow and shut-in periods of the C2 MDT experiments were selected for history matching simulation in the MH Simulator Code Comparison Study [7]. The C2 MDT experiments involved alternating flow periods of various durations, using a positive displacement pump, and build-up phases, during which there was no pumping, as shown in Figure 10.

The pressure and temperature were measured directly during the various flow and buildup periods of the MDT test, while produced fluid volumes were not measured directly. As shown in Figure 10, during the first flow period the bottomhole pressure was kept within the MH stability region, while during the second and third flow periods, the bottomhole pressure was lowered below the MH-gas-water equilibrium pressure, which led to the dissociation of MH.

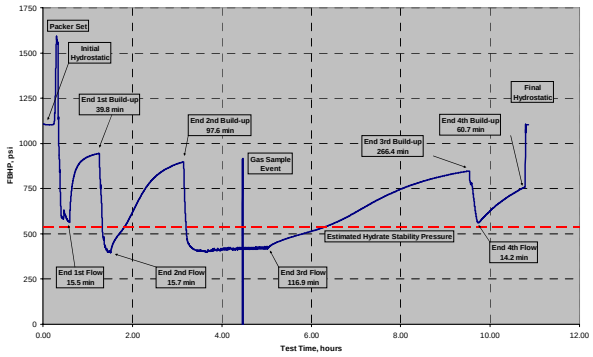

Figure 10: Measured bottomhole pressure

Construction of near wellbore model

Two-dimensional radial reservoir model was constructed for the area of 10 m from the test well with the thickness of 10 m. Thirty-six grid blocks with a minimum grid size (Δr) of 3 mm were allocated in the radial direction, incorporating two innermost grid blocks replicating the wellbore and the MDT tool so as to rigorously simulate the wellbore storage effect as shown in Figure 11. Sixty-six grid layers having a thickness of 15.24 cm were assigned for the vertical direction. The initial reservoir properties such as porosity, water saturation and MH saturation were defined to each grid layer as listed in Table 6.

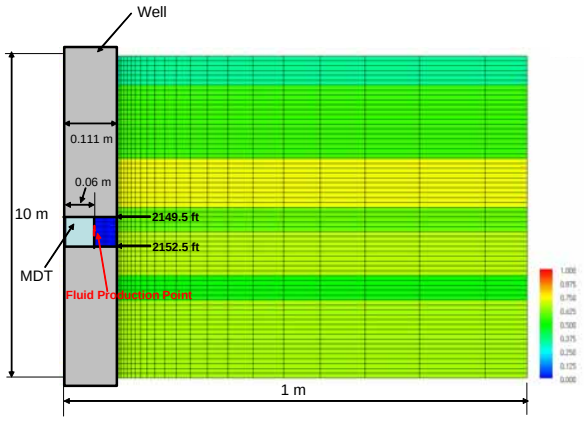

Figure 11: Grid system of the near wellbore model

Parameters	Value
Modeling area	10.1 m around the well
Thickness (m)	10.1
Grid system	r-z radial coordinate
Number of grid blocks	36 (r-direction) 66 (z-direction)
Horizontal absolute permeability (mD)	1,000 (outside well) 100,000 (inside well)
Vertical absolute permeability (mD)	100 (outside well) 100,000 (inside well)
Porosity (%)	29.6-36.7 (outside well) 100.0 (inside well)
Initial pressure (MPa)	6.78 (@model center)
Initial Temperature (K)	275.95 (@model center)
Initial MH saturation (%)	34.9-72.7 (outside well) 0.0 (inside well)
Initial water saturation (%)	27.2-65.1 (outside well) 0.0 (inside well)
Rock compressibility (1/Pa)	1.0×10^{-9}
Gas solubility into water	accounted
MH reformation	neglected

Table 6: Reservoir model parameters

Analysis by numerical simulation

Using the reservoir model constructed in the above, the gas and water production rates and the bottomhole temperature were simulated for the flow periods, specifying the observed bottomhole pressure profile as a boundary condition. On the other hand, the bottomhole pressure and temperature were simulated specifying the fluid flow of zero at the fluid inlet of the MDT tool. Since the bottomhole pressure and temperature performances predicted were significantly different from those observed (Figure 12 (a)), the following parameters were tuned as matching parameters in the course of history matching:

- Initial effective permeability to water (irreducible water saturation for relative permeability calculation)
- Rock compressibility
- Relative permeability to gas
- Gas volume initially dissolved in water phase
- intensity for MH re-formation

As shown in Figure 12 (b), excellent matching was attained between simulated and measured bottomhole pressure. Although the simulated temperature depicted in this figure is slightly different from the observed one, the temperature in the annulus varies by location (depth); namely, the temperature predicted at the upper part of the MDT tool was higher than observed one due to the effect of MH re-formation, while that predicted at the lower part of the MDT tool was much lower than observed one.

Figure 13 shows the gas and water rates at the bottomhole predicted by the history matched model, which indicates that the water production was dominant at the bottomhole conditions even during the third flowing period. The gas and MH saturation distributions at the end of each flowing and shut-in period are depicted in Figures 14 and 15, respectively. It is clarified that most of gas was accumulated not in the reservoir but in the annulus inducing the large wellbore storage effect and that the radius of MH dissociation was as small as about 5 cm from the sand face. Although the initial effective permeability of about 0.12 mD was definitely inferred from the pressure data of the first flow, other interesting parameters such as the radius of MH dissociation, permeability after MH dissociation were not indicated in the bottomhole pressure behavior due to this wellbore storage effect.

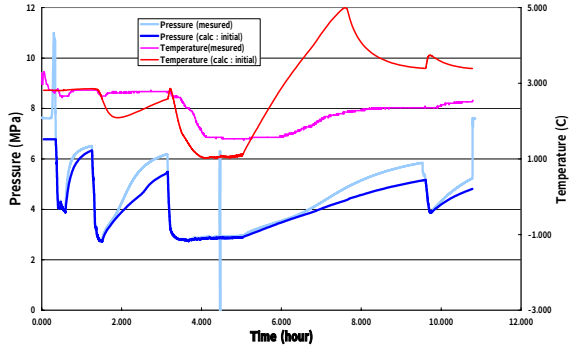

(a) Initial run

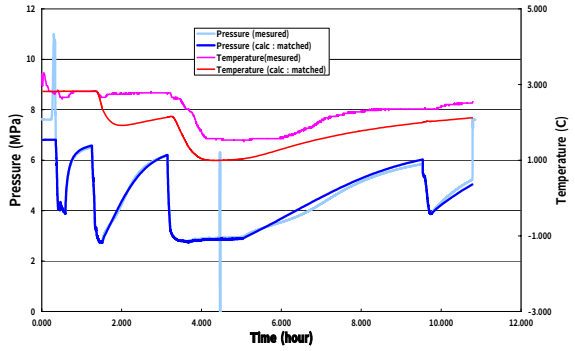

(b) History matched

Figure 12: Simulated bottomhole pressure and temperature behavior

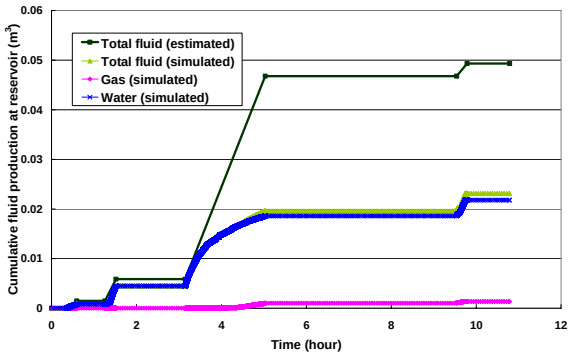

Figure 13: Gas and water rates at the bottomhole predicted by the history matched model

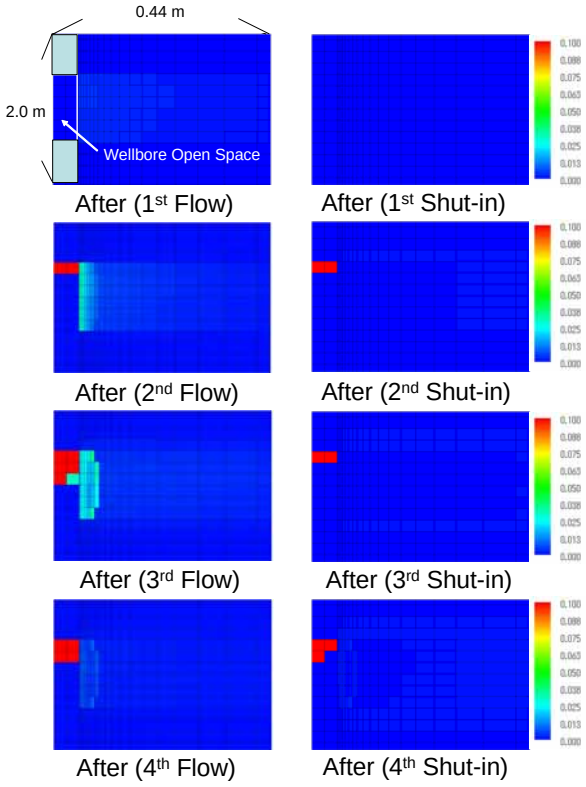

Figure 14: Gas saturation distribution predicted by the history matched model

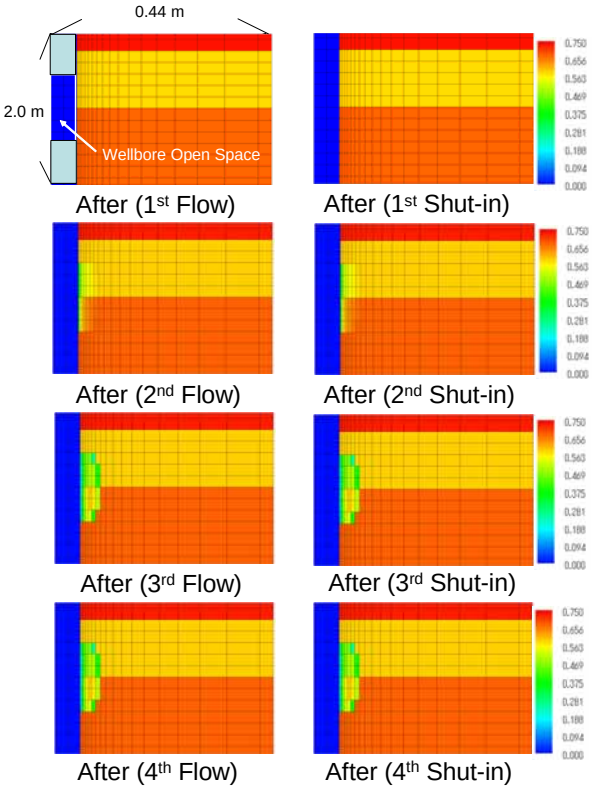

Figure 15: MH saturation distribution predicted by the history matched model

ANALYSES OF PRODUCTION TEST IN MALLIK

As discussed in our paper published in this volume [9], successful history matching was accomplished for reproducing the behavior of 15-hour continuous MH dissociation and production test by depressurization conducted on one of the Mallik MH reservoirs in April 2007. Although the total duration spent for the test was almost the same as that for the above mentioned MDT tests, the radius of MH dissociation was much larger than those by MDT tests, which reduces the well bore storage effect providing more insights into the mechanism for MH dissociation and production.

However, since the flow conditions were not stable in this production test, the fluctuated/scattered data measured during the test made the analysis very complicated, leading to many solutions and hypotheses for the MH dissociation and production mechanism.

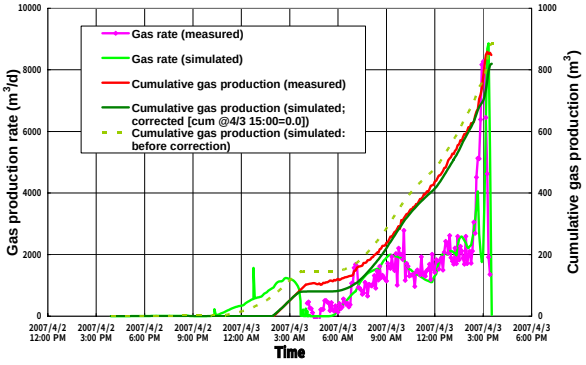

Figure 16: Gas production predicted by the final history matched model

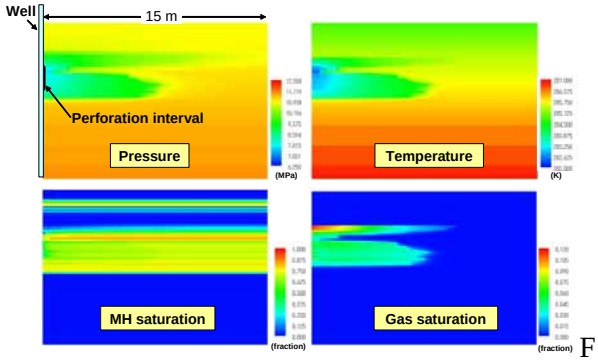

Figure 17: Reservoir properties at the end of the test predicted by he final history matched model

COMPARISON BETWEEN MDT AND PRODUCTION TESTS

The analysis of pressure transient tests in MH reservoirs is imprecise using simplified analytical techniques and may be subject to error due to the large number of uncertainties, such as the distribution of MH saturation near the wellbore and the production rates of water and gas phases during the test period. Moreover, the informative pressure responses to the MH dissociation front at the time of pressure propagation may be masked by the wellbore storage effects and/or errors in semilog type pressure approximation, which makes the analysis more complicated and erroneous. Since a short-term MDT test somehow distorts the system response, a longer test is recommended for a more representative data set.

Taking account of the very low initial effective permeability and the very small area expected for MH dissociation, the durations requested for the pressure transient test, production test and pilot test for MH reservoirs should be totally different from those for a conventional oil and gas reservoir. As summarized in Table 7, it may be necessary to spend a couple of days only for a single MDT test. For a long term production test, it must be the most essential to keep the bottomhole condition as stable as possible. Bottomhole assemblies for the test well should be designed giving the establishment of a stable flow the heist priority.

Well test	Duration for conventional reservoirs	Duration for MH reservoirs
Pressure transient test (RFT, MDT)	5-10 hours	1-2 days
Sort tem flow test (DST, etc.)	1-2 days	5-10 days
Long term production test	1-2 months	1-6 months

Table 7: Test durations requested for various test

CONCLUSIONS

Through the numerical simulation studies for analyzing MDT tests and production test conducted in MH reservoirs, the following insights were obtained for the parameters learned from pressure transient tests.

- The permeability value suggested by the conventional well test analysis methods is close to the average effective permeability to a certain fluid over the region of MH dissociation.

- When initial the initial effective permeability is large enough for the fluid flow, decrease in pressure derivative at the last stage of a test period looks indicating the presence of a constant pressure boundary (CPB).
- When initial effective permeability is very small, pressure derivative may continue to increase even at the last stage of a test period due probably to the insufficient test period. The radius to the composite boundary may suggest the radius to the location in between wellbore and hydrate dissociation front.

The simulation studies also suggested the following as difficulties and limitations of MDT/production tests in MH reservoirs:

- Accurate flow rates of gas and water, which should vary with time, is unknown.
- Distributions of saturation for each phase (water, gas and MH) and hence the saturation dependent parameters such as the relative permeability to each phase, effective viscosity and total compressibility are unknown.
- The time for the pressure propagation to the MH dissociation front is very early. The informative pressure responses at this time are muffled by the wellbore storage effect and/or errors in log-log type pressure approximation.
- Other than the above, pressure behavior affected by the MH dissociation may mislead the analysis.
- For a long term production test, it must be the most essential to keep the bottomhole condition as stable as possible.

ACKNOWLEDGMENTS

This work was financially supported by the Research Consortium for Methane Hydrate Resources in Japan (MH21 Research Consortium) on the National Methane Hydrate Exploitation Program by the Ministry of Economy, Trade and Industry (METI). The authors gratefully acknowledge them for the financial support and permission to present this paper. The authors wish to thank Japan Oil Engineering Company, the University of Tokyo, Japan Oil, Gas and Metals National Corporation, National Institute of Advanced Industrial Science, Geological Survey of Canada, Natural Resources Canada, United States Geological Survey and APA Petroleum Engineering Inc. for their technical support.

REFERENCES

[1] Dallimore SR, Collett TS, Uchida T, Weber M. *Overview of the science program for the Mallik 2002 Gas Hydrate Production Research Well Program; in Scientific Results from the Mallik 2002 Gas Hydrate Production Research Well Program, Mackenzie Delta, Northwest Territories, Canada*, In: S.R. Dallimore, T.S. Collett, editor. Scientific Results from the Mallik 2002 Gas Hydrate Production Research Well Program, Mackenzie Delta, Northwest Territories, Canada, Geological Survey of Canada Bulletin 585, 2005.

[2] Satoh T, Dallimore SR, Collett TS, Inoue T, Hancock SH, Moridis G, Weatherill B. *Production-test planning for the JAPEX/JNOC/GSC et al. Mallik 5L-38 gas hydrate production research well; in Scientific Results from the Mallik 2002 Gas Hydrate Production Research Well Program, Mackenzie Delta, Northwest Territories, Canada*, In: S.R. Dallimore, T.S. Collett, editor. Scientific Results from the Mallik 2002 Gas Hydrate Production Research Well Program, Mackenzie Delta, Northwest Territories, Canada, Geological Survey of Canada Bulletin 585, 2005.

[3] Hancock SH, Dallimore SR, Collett TS, Carle D, Weatherill B, Satoh T, Inoue T. *Overview of pressure-drawdown production-test results for the JAPEX/JNOC/GSC et al. Mallik 5L-38 gas hydrate production research well; in Scientific Results from the Mallik 2002 Gas Hydrate Production Research Well Program, Mackenzie Delta, Northwest Territories, Canada*, In: S.R. Dallimore, T.S. Collett, editor. Scientific Results from the Mallik 2002 Gas Hydrate Production Research Well Program, Mackenzie Delta, Northwest Territories, Canada, Geological Survey of Canada Bulletin 585, 2005.

[4] Earlougher RC Jr. *Advances in Well Test Analysis*, Society of Petroleum Engineers of AIME, Dallas, Texas, Monograph 5, 1977.

[5] Sabet MA. *Well Test Analysis*, Gulf Professional Publishing Co., Houston, Texas, Contributions in Petroleum Geology and Engineering, Volume 8, 1991.

[6] Kurihara M, Funatsu K, Kusaka K, Yasuda M, Dallimore SR, Collett TS, Hancock SH. *Well-test analysis for gas hydrate reservoirs: examination of parameters suggested by conventional analysis for the JAPEX/JNOC/GSC et al. Mallik 5L-38 gas hydrate production research well*, In: S.R. Dallimore, T.S. Collett, editor. Scientific Results from the Mallik 2002 Gas Hydrate Production Research Well Program, Mackenzie Delta, Northwest Territories, Canada, Geological Survey of Canada Bulletin 585, 2005.

[7] Anderson BJ, Wilder J, Kurihara M, White M, Moridis G, Wilson S, Pooladi-Darvish M, Masuda M, Collett TS, Hunter R, Narita H, Rose K, Boswell R. *Analysis of Modular Dynamic Formation Test Results from the "Mount Elbert" stratigraphic test well, Milne Point, Alaska*, Proceedings of the 6th International Conference on Gas Hydrates, Vancouver, CANADA 2008.

[8] Numasawa M, Dallimore SR, Yamamoto K, Yasuda M, Imasato Y, Mizuta T,. Kurihara M, Masuda Y, Fujii T, Fujii K, Wright JF, Nixon FM, Cho B, Ikegami T, Sugiyama H. *Objectives and Operation Overview of the JOGMEC/NRCan/Aurora Mallik Gas Hydrate Production Test*, Proceedings of the 6th International Conference on Gas Hydrates, Vancouver, CANADA 2008.

[9] Kurihara M, Funatsu K, Ouchi H, Masuda Y, Yasuda M, Yamamoto K, Numasawa M, Fujii T, Narita H, Dallimore SR, Wright JF. *Analysis of the JOGMEC/NRCan/Aurora Mallik Gas Hydrate Production Test through Numerical Simulation*, Proceedings of the 6th International Conference on Gas Hydrates, Vancouver, CANADA 2008.

[10] Masuda Y, Konno Y, Iwama H, Kawamura T, Kurihara M, Ouchi H. *Improvement of Near Wellbore Permeability by Methanol Stimulation in a Methane Hydrate Production Well*, Paper OTC 19433 presented at 2008 Offshore Technology Conference held in Houston, Texas, U.S.A., 5–8 May 2008.

[11] Kurihara M, Ouchi H, Inoue T, Yonezawa T, Masuda Y, Dallimore SR, Collett TS. *Analysis of the JAPEX/JNOC/GSC et al. Mallik 5L-38 gas hydrate thermal-production test through numerical simulation*. In: S.R. Dallimore, T.S. Collett, editor. Scientific Results from the Mallik 2002 Gas Hydrate Production Research Well Program, Mackenzie Delta, Northwest Territories, Canada, Geological Survey of Canada Bulletin 585, 2005.

[12] Masuda Y, Naganawa S, Ando S, Sato K. *Numerical calculation of gas-production performance from reservoirs containing natural gas hydrates*. Paper SPE 38291, Proceedings of Western Regional Meeting, Long Beach, California, 1997.

[13]Masuda Y, Fujinaga Y, Naganawa S, Fujita K, Sato K, Hayash, Y. *Modeling and experimental studies on dissociation of methane gas hydrates in Berea sandstone cores*. Presented at 3rd International Conference on Gas Hydrates, Salt Lake City, Utah, 1999.

[14] Aziz K, Settari, A. *Petroleum Reservoir Simulation*, Applied Science Publishers Ltd. (Chapman & Hall), London, United Kingdom, 1979.